Digital Communications and Networks 9 (2023) 698–709

Contents lists available at ScienceDirect

Digital Communications and Networks

journal homepage: www.keaipublishing.com/dcan

Wi-Wheat+: Contact-free wheat moisture sensing with commodity WiFi based on entropy

Weidong Yang [a,*], Erbo Shen [b,c], Xuyu Wang [d], Shiwen Mao [e], Yuehong Gong [a], Pengming Hu [a]

[a] College of Information Science and Engineering, Henan University of Technology, Zhengzhou, 450001, China
[b] Henan Key Laboratory of Grain Photoelectric Detection and Control, Zhengzhou, 450001, China
[c] College of International Education, Kaifeng University, Kaifeng, Henan, 475004, China
[d] Knight Foundation School of Computing & Information Sciences, Florida International University, Miami, FL, 33199, USA
[e] Department of Electrical and Computer Engineering, Auburn University, Auburn, AL, 36849-5201, USA

ARTICLE INFO

This work was presented in part at 2018 IEEE International Conference on Communications, Kansas City, MO, May 2018 [16].

Keywords:
Channel state information (CSI)
WiFi
Multi-scale entropy
Multi-class support vector machine (SVM)
Radio frequency (RF) sensing

ABSTRACT

In this paper, we propose a contact-free wheat moisture monitoring system, termed Wi-Wheat+, to address the several limitations of the existing grain moisture detection technologies, such as time-consuming process, expensive equipment, low accuracy, and difficulty in real-time monitoring. The proposed system is based on Commodity WiFi and is easy to deploy. Leveraging WiFi CSI data, this paper proposes a feature extraction method based on multi-scale and multi-channel entropy. The feasibility and stability of the system are validated through experiments in both Line-Of-Sight (LOS) and Non-Line-Of-Sight (NLOS) scenarios, where ten types of wheat moisture content are tested using multi-class Support Vector Machine (SVM). Compared with the Wi-Wheat system proposed in our prior work, Wi-Wheat+ has higher efficiency, requiring only a simple training process, and can sense more wheat moisture content levels.

1. Introduction

In the food industry, harvested grains need to be stored safely to meet the future food demand, particularly, to deal with urgent demands when there is a disaster or famine. Grain storage may be accomplished safely by controlling two important physical conditions: temperature and moisture content [1]. The moisture content indicates whether they are harvested and stored safely, and moisture content is one of the food quality and safety criteria in grain trading [2]. Detection of grain moisture is considerably different in different stages of the grain distribution chain from producer and consumer. Since the standard reference methods for determining the moisture content level of grains usually involve time-consuming laboratory procedures and a long drying cycle in the oven, rapid and nondestructive moisture content determination is essential for safe grain storage [3].

The existing grain moisture content determination methods can be divided into two categories: destructive methods and non-destructive methods [4–12]. Existing destructive methods require oven drying for a specific duration of time at a specific temperature. One of the most commonly used destructive methods is to determine the amount of water lost by evaporating all the water in the crushed quantitative sample at a slightly higher temperature (105 °C). Such methods are not suitable for general use in the grain trade because they are tedious and time-consuming. Meanwhile other faster testing methods have been developed. One example of non-destructive detection is putting the sample into an oven at 130 °C for 19 h according to the American Society of Agricultural and Biological Engineers (ASABE) standard, with the difference between before and after measurement being the moisture content. As information technology has developed, more advanced methods have been developed. Using the magnetic or electric properties method as an example, such non-destructive methods are less time-consuming and require less man power because grain or food items can be used directly without any processing, such as cleaning or crushing. However, detection devices for non-destructive methods are usually complex and expensive.

With significant advancements in wireless communications and

* Corresponding author.
E-mail addresses: yangweidong@haut.edu.cn (W. Yang), shenbo412@qq.com (E. Shen), xuywang@fiu.edu (X. Wang), smao@ieee.org (S. Mao), yuehonggong@163.com (Y. Gong), 337370004@qq.com (P. Hu).

https://doi.org/10.1016/j.dcan.2022.03.014
Received 27 June 2021; Received in revised form 14 March 2022; Accepted 18 March 2022
Available online 23 March 2022

Radio Frequency (RF) sensing [13,14], RF signals have been exploited for various sensing applications. For example, Channel State Information (CSI) data may now be recovered readily from off-the-shelf WiFi Network Interface Cards (NIC), such as the Intel WiFi Link 5300 NIC. CSI can provide fine-grained channel information, which carries rich channel characteristics such as multi-path effects, distortion, and shadowing fading. Furthermore, CSI amplitude and phase difference data are far more stable than the Received Signal Strength (RSS). As a result, fall detection, activity recognition, respiratory and heart rate monitoring, and indoor positioning have all been successfully developed using CSI-based sensing, detection, and recognition technologies [14,15]. In this study, we propose to use WiFi CSI data for contact-free wheat moisture monitoring, motivated by the existing CSI sensing techniques and the ease of access with commodity WiFi.

To distinguish it from the Wi-Wheat system proposed in our prior work, we present a non-destructive and low-cost wheat moisture sensing system using commodity WiFi, named Wi-Wheat+. The proposed system does not require any complex or dedicated devices, thus having a low-cost and being easy to deploy. The main contributions made in this paper are summarized as follows.

- We validate the feasibility of utilizing the fine-grained CSI amplitude information entropy to detect wheat moisture level. To the best of our knowledge, this is the first study that uses CSI data for contact-free detection of wheat moisture content level.
- To produce a highly accurate prediction of wheat moisture, we propose a novel algorithm called the Multi-Channel and Multi-Scale Entropy (MCSEn) algorithm, which is combined with a machine learning algorithm called Multi-class Support Vector Machine (SVM).
- We designed and implemented the Wi-Wheat+ system, which includes the CSI data acquisition module, the CSI data processing module, and a wheat moisture sensing module. Two notebook computers equipped with commercial WiFi cards are used for WiFi CSI data acquisition. Another computer executes the algorithm of MCSEn combined with Multi-class SVM to process the collected WiFi CSI data for moisture level detection.
- To validate the performance of the proposed Wi-Wheat+ system, we conduct extensive experiments with stored wheat samples. The experiment results show that Wi-Wheat+ can achieve considerably high classification accuracy in both Line-Of-Sight (LOS) and Non-Line-Of-Sight (NLOS) scenarios.

The remainder of this paper is organized as follows. Section 2 reviews relevant studies, and Section 3 presents preliminaries. Section 4 describes the Wi-Wheat+ system design, while Section 5 evaluates its performance. Section 6 concludes this paper.

2. Related work

2.1. Wheat moisture measurement

Existing methods for wheat moisture measurement can be classified into the following: the drying method [5], the capacitance method [6], the resistance method [7], the microwave method [9,10], and the neutron gauge method [11]. In practice, the oven-drying method [5] is extensively used. Although this method is highly accurate, it is only suitable for laboratory environments and does not meet the requirements of online moisture detection in the field. The capacitive moisture detection method [6] is also widely used, but its performance is limited by the fact that the measurement values are sensitive not only to temperature, but also to grain flow velocity and grain compactness in the dryer. Moreover, grain moisture measurement values might be influenced by a variety of other factors. Consequently, this method requires one to recalibrate the capacitive sensors after using the system for a certain period of time.

As an example of resistance methods, an online resistance grain moisture detector was proposed in Ref. [7] based on the model on the relationship between measurement frequency and grain moisture as well as the nonlinear temperature correction method. The detector consists of two computers. Based on Voltage-to-Frequency (V/F) conversion, one computer detects grain resistance values. The other computer is focused on moisture and frequency conversion, as well as nonlinear temperature correction. Microwave [9,10] and neutron [11] methods have various advantages, such as high accuracy, fast detection speed, non-destructive, and noninvasive measurements. Furthermore, they can easily determine the grain's internal moisture. However, the measurement equipment required for these methods is usually complex and expensive.

The microwave method, which uses the microwave principle to determine moisture content, has gained increasing interest in recent years. This method exploits change in microwave signal after penetrating the sample material. It has been shown that the received signal can well capture the material's characteristics. Nelson et al. applied this idea and proposed a method that utilizes the dielectric constant and loss factor [17]. This method achieves a high degree of accuracy. However, this method requires tuning the parameters of equipment, and the measurement of dielectric constant is complex and costly, which hinders its wide development.

2.2. CSI-based RF sensing systems

Indoor localization, wheat mildew detection [38], and device-free RF sensing [14,15] have all made extensive use of CSI-based sensing systems and have been widely used. For example, the FIFS [18] and DeepFi [19] systems employ CSI amplitude values for indoor localization; the PhaseFi [20] system exploits calibrated CSI phase data; and the BiLoc system [21] and ResLoc system [22] incorporate bimodal CSI data for indoor localization using deep learning models. Moreover, the CiFi system considers phase difference values for indoor localization, where a deep convolution network is incorporated for learning the CSI data in the image form, for achieving high localization accuracy and reducing the data storage requirement [23].

On the other hand, CSI-based contact-free sensing systems are widely used in a variety of applications such as activity recognition, fall detection, and vital sign monitoring. For activity recognition, the E-eyes system [24] implemented a device-free location-oriented method for recognizing household activities based on CSI amplitude. For recognizing spoken words, the WiHear system [25] exploited specialized directional antennas to measure CSI variations caused by lip movements. The CARM system [26] incorporated a CSI-based speed model as well as an activity model for identifying the relationship between human activity and CSI dynamics. For fall detection, WiFall [27] and RT-Fall [28] utilized CSI amplitude and phase differences, respectively, to detect the fall of certain objects. For vital sign monitoring, PhaseBeat [29] and TensorBeat [30] employed CSI phase differences to estimate a single or multiple subjects' respiration rates. In recent works Wi-Fire [31] and Wi-Metal [32], the authors utilized CSI data to detect fire events and metal objects, respectively. In order to design a universal scheme for determining whether there is a line-of-sight (LOS) path in the multi-path propagation environment, Zhou et al. implemented a visual range recognition system [33], termed LiFi, based on a statistical method using commercial WiFi equipment.

The Wi-Wheat system proposed in our previous study is designed to sense the anomaly moisture level in wheat samples [16], which utilizes CSI phase difference and CSI amplitude as features to detect only two kinds of wheat moisture content. A higher resolution of moisture detection ability would be required for an online system. As a result, in this paper, we propose the Wi-Wheat+ system, which uses the Intel 5300

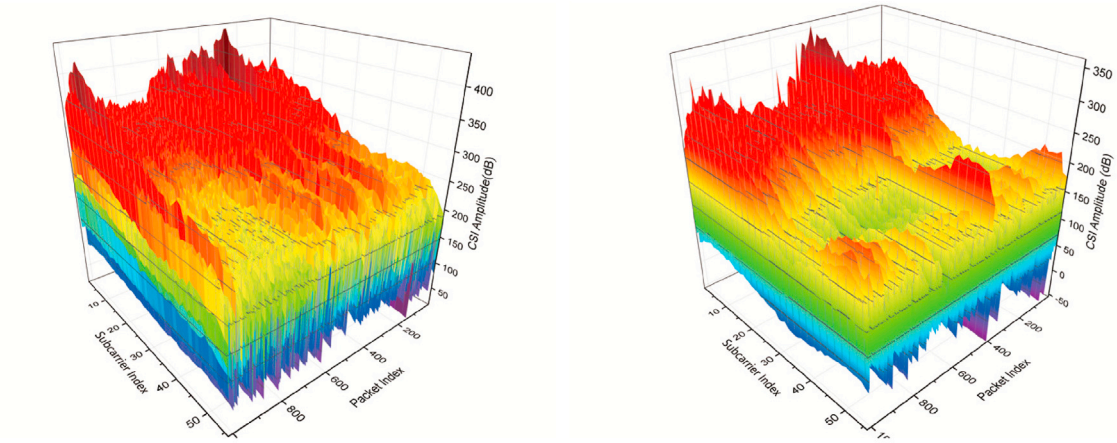

(a) CSI data sampled in the LOS scenario (b) CSI data sampled in the NLOS scenario

Fig. 1. CSI data collected from the LOS and NLOS cases.

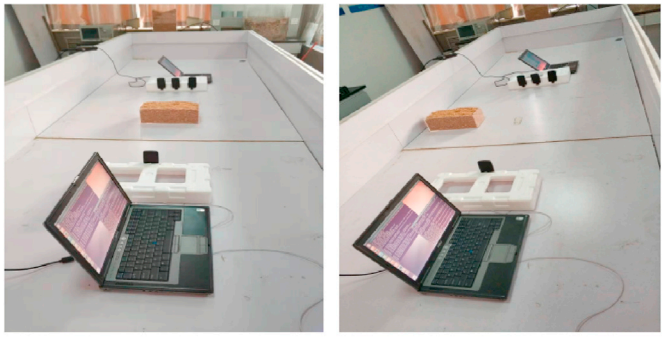

(a) The LOS scenario (b) The NLOS scenario

Fig. 2. Two experimental scenarios, LOS and NLOS, for evaluating the performance of the proposed algorithms.

wireless network interface card and a customized device driver to acquire Channel Frequency Response (CFR) information in the form of CSI. Wi-Wheat+ senses the changes in wheat moisture content and predict more kinds of wheat moisture levels. When compared with our earlier study, this system can sense more moisture content levels, the proposed MCSEn features are more effective, and the Multi-Class SVM machine learning model is more computationally efficient than the deep learning model (i.e., LSTM) used in our prior work [34].

3. Preliminaries and feasibility

Orthogonal Frequency Division Multiplex (OFDM) has been adopted in most modern communication systems such as Long Term Evolution (LTE) and WiFi. To deal with frequency selective fading, in OFDM, a channel (with 20 MHz or 40 MHz bandwidth as in IEEE 802.11n) is divided into multiple orthogonal subcarriers to cope with frequency selective fading. In recent years, OFDM has been applied to indoor localization as well as other RF sensing applications [19,20]. Rich CSI data is usually available from open source device drivers, which can be exploited for RF sensing. Such CSI data can help to quantify the state information of different subcarriers on each antenna, and has the advantages of higher stability, higher sensitivity, and higher resolution than RSS.

The OFDM system can be represented by the following model as

$$Y = H \cdot X + n \tag{1}$$

where X and Y represent the transmitted signal vector and the received signal vector, respectively, H represents the channel gain matrix (i.e., the CSI), and n represents the additive noise introduced by the channel. The subcarriers of the WiFi Physical Layer (PHY) in the 2.4 GHz or 5 GHz bands can be regarded as narrow band flat fading channels that are sufficiently stable for RF sensing. The frequency response of the ith subcarrier can be expressed as

$$h_i = |h_i| \exp\{j \angle h_i\} \tag{2}$$

where $|h_i|$ and $\angle h_i$ are the ith subcarrier's amplitude and phase, respectively. In this research, the Wi-Wheat+ system will leverage the CSI amplitude and its data entropy for contact-free detection of wheat moisture content level. The device driver for the Intel WiFi Link 5300 NIC (which implements the IEEE 802.11n standard) can provide CSI information from 56 subcarriers. Examples of the captured CSI data are plotted in Fig. 1 for both the LOS and NLOS scenarios.

As shown in Fig. 2, in the two experiment scenarios, the plexiglass box is filled with wheat samples and placed between the receiving antenna and the transmitting antenna, such that the LOS path between the transmitter and receiver is blocked. The proposed Wi-Wheat+ system captures the CSI from the 56 WiFi channel subcarriers using three receiving antennas. The three-dimensional diagrams in Fig. 1 present the original CSI amplitude data in decibels (dB) sensed by the proposed system, for different subcarriers and different received WiFi packets. The CSI data for wheat samples with the same moisture content, have a similar shape but the amplitudes in the LOS and NLOS scenarios differ.

In Fig. 3, we also plot the CSI amplitude data for the 56 subcarriers collected from three different antennas. Because the trends of the curves are comparable in both the LOS and NLOS scenarios, it is evident that there are coincidence points, which mean the amplitude values from different antennas are equal for some of the subcarriers. It can be concluded that, for the same wheat moisture level, the CSI amplitude data sampled from different antennas is correlated to the same wheat moisture level.

Furthermore, Figs. 4 and 5 present a comparison of CSI amplitude and phase difference for various wheat moisture levels. To further verify the correlation between wheat moisture content and CSI data, we set 13% as a wheat moisture content reference for anomaly detection, i.e., a wheat moisture level below or above this value is considered abnormal. As shown in Fig. 4, we begin using CSI amplitude as the feature for the comparison study. It can be seen from Fig. 4(a) that there is no obvious difference between wheat moisture levels 11% and 13%, and there is a slight difference between wheat moisture levels 13% and 14.7%, as shown in Fig. 4(b). However, there is a big difference between wheat moisture levels 13% and 16.5%, as shown in Fig. 4(c). Then, as the feature for the comparison study, we use CSI phase difference, which is computed as the difference between the two phase samples collected

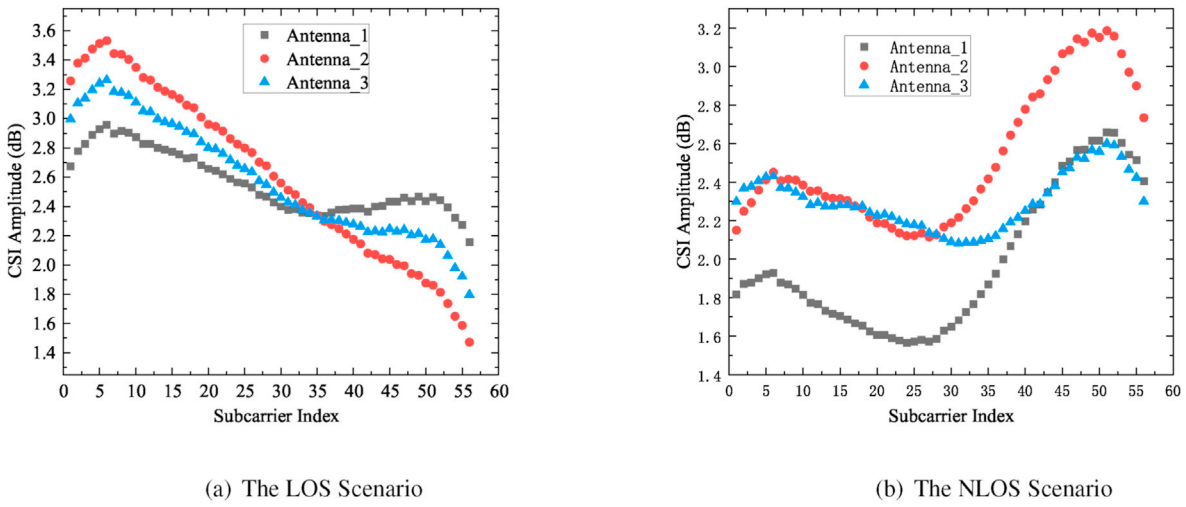

Fig. 3. CSI amplitude measured from three different receiving antennas in the LOS and NLOS cases.

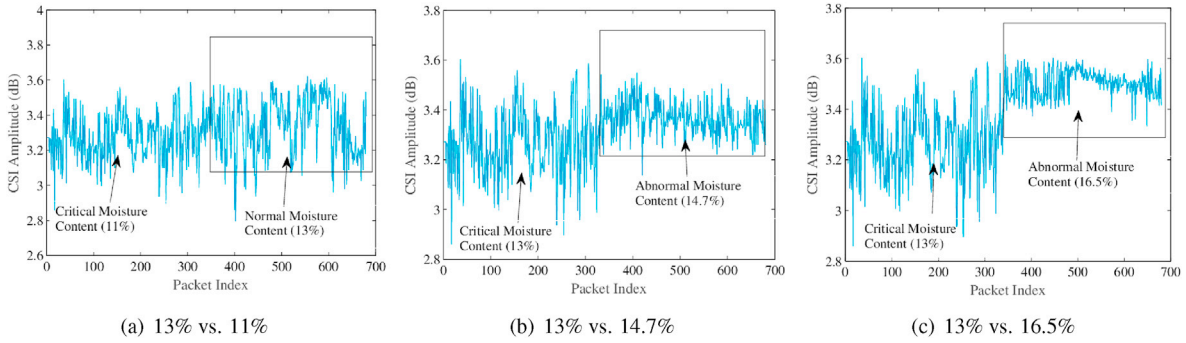

Fig. 4. CSI amplitude comparison for different wheat moisture levels.

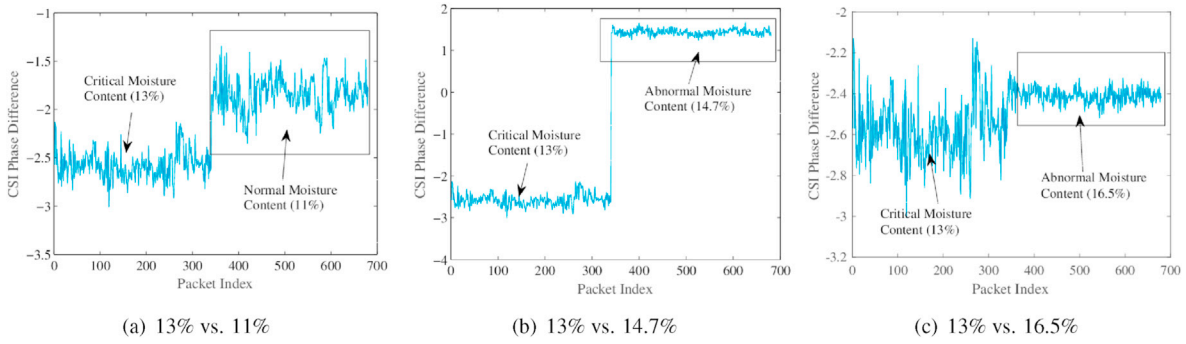

Fig. 5. CSI phase difference comparison for different wheat moisture levels.

from two antennas on the same subcarrier. Fig. 5 shows the results plotted. It is clear that the CSI phase difference between 13% and 11%, 13% and 14.7%, and 13% and 16.5% is significantly different. These results validate the correlation between wheat moisture level and WiFi CSI amplitude and phase difference data, as well as the feasibility of detecting wheat moisture level using WiFi CSI data.

4. Design of the Wi-Wheat+ system

4.1. Architecture

The Wi-Wheat+ system architecture is illustrated in Fig. 6, which includes three major components: (i) CSI Sensing, (ii) CSI Data Processing, and (iii) a Multi-class SVM. For CSI data sensing, we leverage two mobile devices (e.g., laptops) equipped with the Intel WiFi link 5300 NIC, one as a transmitter and the other as a receiver. The transmitter is configured to operate in the *injection* mode while the receiver is set in the *monitoring* mode. With each received packet, the receiver NIC senses CSI data via the device driver, whilst the transmitter sends a number of packets to the receiver. The CSI data processing section mainly consists of two modules: the signal pre-processing and the data feature extracting modules. The CSI pre-processing module of Wi-Wheat+ is comprised of outlier detection, data normalization, and noise removal modules. The multi-scale entropy is computed from CSI data via the CSI data feature extracting module. Using the multi-scale entropy of CSI data, the Multi-class SVM classifies wheat samples into 10 different moisture levels.

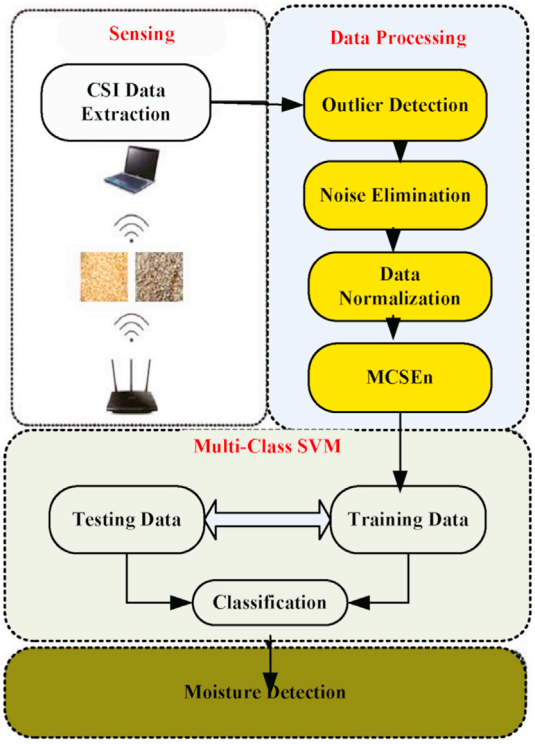

Fig. 6. The Wi-Wheat+ system architecture.

The design of the three principal components is discussed in detail in next section.

4.2. CSI data pre-processing

The three components of the data pre-processing module are designed as follows.

Outlier Detection: The captured CSI data is usually noisy with abnormal samples. Outlier detection is performed to detect bad data samples in the raw CSI data sequence that should be replaced with a valid value. To detect and remove outliers, we use the Pauta criterion method. The detailed process is presented as follows.

Step 1: Let $\{X_i\}, i = 1, 2, \ldots, n$ be the series of CSI amplitude or phase difference sampled from a subcarrier. The arithmetic mean of the samples is given by

$$\overline{X} = \frac{1}{n}\sum_{i=1}^{n} X_i \tag{3}$$

Step 2: The residual V_i and the standard deviation σ are calculated by (4) and (5), respectively.

$$V_i = X_i - \overline{X}, \quad i = 1, 2, \ldots, n \tag{4}$$

$$\sigma = \sqrt{\frac{1}{n-1}\sum_{i=1}^{n}(X_i - \overline{X})^2} \tag{5}$$

Step 3: For all X_i, $i = 1, 2, \ldots, n$, if $|V_i| \rangle 2.5\sigma$, X_i will be regarded as an abnormal value, and will be replaced by the arithmetic mean value X.
Step 4: Repeat the above 3 steps till all the samples are examined.

Noise Elimination: Next we apply the magnitude-squared Chebyshev Type II filter to mitigate the environmental noise. The response function of the Chebyshev Type II filter is given by

$$|H(j\omega)|^2 = \frac{\varepsilon^2 C_N^2(\omega_s/\omega)}{1 + \varepsilon^2 C_N^2(\omega_s/\omega)} \tag{6}$$

where $\varepsilon \in (0, 1)$ represents the amplitude frequency ripples in the stop band, ω_s is the frequency scaling constant, and N represents the order number of the polynomial $C_N^2(\omega_s/\omega)$, which is given by

$$C_N(x) = \begin{cases} \cos\left(N\cos^{-1}(x)\right), & \text{if } |x| \le 1 \\ \cosh\left(N\cosh^{-1}(x)\right), & \text{if } |x| > 1 \end{cases} \tag{7}$$

Data Normalization: In order to improve the detection accuracy, the input data should be normalized to the range [0, 1] for classification with the SVM. The normalized value Y_i is computed by

$$Y_i = \frac{X_i - \overline{X}}{X_{max} - X_{min}} \tag{8}$$

where X_i represents the raw data, X is the average, and X_{max} and X_{min} represent the maximum and minimum values over a period of time after outlier removal.

4.3. Multi-channel and multi-scale entropy

Entropy is a useful metric in statistics to evaluate the level of regularity or unpredictable variations in a time-series. It is widely used in various fields, such as body state detection for disease diagnosis. However, in complex cases such as CSI data, a single scale entropy may not accurately capture the fluctuations in the signal [37]. Traditional algorithms are usually single-scale based and hence may not be sufficient to account for the multiple timescales inherent in physiological systems. As a result, in Wi-Wheat+, we propose a Multi-channel and Multi-scale Entropy (MCSEn) method for wheat moisture level detection, which exploits the concept of entropy and utilizes the CSI data from 56 subcarriers of the WiFi channel. In particular, we consider the CSI data as a complex one-dimensional time series and extract the CSI signal features to predict wheat moisture content level. The following is description of the procedure.

Step 1: Scaling MCSEn can be computed from different types of entropy from multiple coarse-grained sequences. The time series data is selected from the experiment data, denoted by $\{X_i, i = 1, 2, \ldots, n\}$. The original time series is divided into non-overlapping windows of length t, which is defined as the *scaling factor*. The data samples within each window are then averaged. Each element of the coarse-gained time series Y_t is calculated by

$$Y_t = \frac{1}{t}\sum_{i=(j-1)t+1}^{jt} X_i, \quad 1 \le j \le \frac{N}{t} \tag{9}$$

Step 2: Reconstruction Assume an initial time series $\{X_i, i = 1, 2, \ldots, n\}$. We obtain the following matrix after reconstructing the data space of the time series.

$$X = \begin{bmatrix} X(1) & X(1+t) & \ldots & X(1+(m-1)t) \\ X(2) & X(2+t) & \ldots & X(2+(m-1)t) \\ \vdots & \vdots & \ddots & \vdots \\ X(K) & X(K+t) & \ldots & X(K+(m-1)t) \end{bmatrix} \tag{10}$$

where m stands for the embedded dimensions and $K = n - (m-1)t$. Each row in the above matrix is a reconstructed component, while each column stands for the total reconstructed components with length K. Take reconstructed component j for example, which is given by $\{X(j), X(j+t), \ldots, X(j+(m-1)t)\}$. We reorder the elements from small to large, and set index values $\{j_1, j_2, \ldots, j_m\}$ before reconstructing the components as $X(i+(j_1-1)t) \le \ldots \le X(i+(j_m-1)t)$.

Step 3: Computing MCSEn We first compute $B_i^m(r)$, for all i, using the following equation.

$$B_i^m(r) = \frac{\text{Number of } X(j)\text{'s satisfying } d_j \le r}{N-m} \tag{11}$$

where d_j is the distance between vectors $X(i)$ and $X(j)$, given by $d_j = |X(i), X(j)|, \ i \ne j$, and r is a measure of similarity, which, generally, can be determined by experience. In this paper, we set $r = 0.25 \times \text{std}(X)$, where $\text{std}(\cdot)$ is the standard deviation. The average of $B_i^m(r)$ is then computed as

$$B^m(r) = \frac{\sum_{i=1}^{N-m+1} B_i^m(r)}{N-m+1} \tag{12}$$

and finally, the MCSEn is computed by

$$\text{MCSEn} = -\ln\left|\frac{B^{(m+1)}(r)}{B^m(r)}\right| \tag{13}$$

4.4. Multi-class SVM

In our prior work [16], we applied SVM using CSI data, which is known as binary classification. We can distinguish wheat samples with abnormal moisture levels from those having normal moisture levels. In this study, we randomly divide the processed data into three groups for model training and testing, aiming to find a hyperplane in the n-dimensional data space. We designed a multi-class SVM algorithm to distinguish between 10 different moisture content levels. This method is known as the one-against-the-rest approach [35]. The algorithm procedure is outlined below.

The first step is to construct M binary SVMs, one for each class of moisture level. By solving the following quadratic programming problem, the ith binary SVM is constructed to separate a class i from the other $(M-1)$ classes.

$$\min_{w^i, b^i, \xi^i} \ \frac{1}{2}(w^i)^T w^i + C\sum_{t=1}^{N} \xi_t^i \tag{14}$$

$$\text{s.t.} \ \ (w^i)^T \ O(X_t) + b^i \ge 1 - \xi_t^i, \quad \text{if } y_t = i \tag{15}$$

$$(w^i)^T \ O(X_t) + b^i \ge -1 + \xi_t^i, \quad \text{if } y_t \ne i \tag{16}$$

$$\xi_t^i \ge 0 \tag{17}$$

where the subscript t is the index of samples and the superscript $i \in \{1, 2, \ldots, M\}$ is the class index. A total of M binary SVMs are trained by solving the above quadratic programming problem with n variables.

The decision function is given by

$$f(X_{new}) = \arg\max_{i \in \{1,2,\cdots M\}} \left\{ \sum_{sv} y_t \alpha_t^i \kappa\langle X_t, X_{new}\rangle + b^i \right\} \tag{18}$$

where sv represents the support vectors and $\kappa\langle\cdot,\cdot\rangle$ is the kernel function. If a new sample data X_{new} achieves the largest $f(x)$, then X_{new} will be classified as class i. We collect CSI data from the 56 subcarriers and obtain the entropy values for 10 different moisture content levels, which are subsequently used as feature to predict the moisture level of new wheat samples. Because of the complex indoor propagation environment, the samples are not linearly separable. In order to address this problem, the Gaussian Radial Basis Function (RBF) is adopted as the kernel function to map the processed CSI data into a high-dimensional feature vector space. The RBF kernel function $\kappa\langle\rangle$ is given by

$$K\langle x^{(i)}, x\rangle = \exp\left\{ -\frac{1}{2\sigma^2}\left|\left|x - x^{(i)}\right|\right|^2 \right\} \tag{19}$$

where σ is the standard deviation.

In the multi-class method (for M classes), a binary class SVM classifier

is used to classify each class from all the other classes, and M classification functions are used. Each unidentified sample is classified into one of the M classes according to the largest classification function value. In theory, 10 types of samples can be classified by using 9 binary SVMs. However, in order to improve the accuracy, 10 binary SVMs are used in Wi-Wheat+. The detailed algorithm is presented in Algorithm 1.

Algorithm 1. The Multi-class SVM Algorithm

1 Create training and testing datasets, which should be constructed at the same time and selected randomly;
2 Data normalization: the feature input is normalized to the range of [0, 1];
3 Select the kernel function and parameters of the SVM: the Gaussian RBF is chosen as the kernel function;
4 The SVM is trained using the samples in the training dataset, using the LIBSVM toolbox [36];
5 The trained model is now ready for the classification of new wheat data;

5. Experimental results and discussions

Fig. 2 presents the two scenarios considered in our experimental study. In a computer laboratory environment, CSI data is measured in both LOS and NLOS scenarios. The Wi-Wheat+ system was developed using off-the-shelf laptops and WiFi NICs. The system consists of an HP ProBook 4411s laptop with a 2.1 GHz Intel (R) Pentium 2 CPU and 2 GB of RAM serving as the receiver, and a Sony PCG-6S1T laptop serving as the transmitter. Both laptops come with the Ubuntu 12.04 operating system and are equipped with the Intel Link 5300 WiFi NIC. To capture 5 GHz CSI data, we set the transmitter to the injection mode and the receiver to the monitor mode. The transmitter uses one antenna to transmit WiFi packets, and the receiver uses three antennas to receive the WiFi packets. CSI data is extracted for each received packet at the receiver side.

It is worth noting that Wi-Wheat+ is different from our prior work [16] in feature extraction. The Entropy of the time series captured from each subcarrier (56 in total, each with 1000 samples), termed MCSEn, is extracted. We have shown that such characteristics can accurately represent the properties of wheat at different moisture contents. We will demonstrate its performance with experiments in this section.

5.1. Adjusting wheat sample moisture level

We next describe the process of how to adjust the wheat moisture level. Assume M_{target} is the target moisture level, and $M_{target} \in \{8\%, 9\%, 10\%, 11\%, 12\%, 13\%, 14\%, 15\%, 16\%, 17\%\}$. The specific steps of the procedure are as follows.

Step 1: We first expose the wheat sample to the sun for 72 h to obtain a wheat sample with a base moisture content of 8.2%.
Step 2: The target moisture level is calculated by

$$M_{target} = \frac{W_{target} M_{base} + \Delta w}{W_{target} + \Delta w} \tag{20}$$

where W_{target} is the weight of wheat to be adjusted (i.e., 2.8 Kg), M_{base} is the base moisture content, which is 8.2%, and Δw denotes the amount of water to be added, given by

$$\Delta w = \frac{W_{target}(M_{target} - M_{base})}{1 - M_{target}} \tag{21}$$

By adding different amounts of water Δw to the wheat samples, 10 sets of wheat samples are obtained this manner.

Step 3: We seal the 10 sets of wheat samples into fresh-preserving bags and put them in a refrigerator at a temperature of 4 °C for 72 h. The wheat samples are then left at room temperature for 48 h, during which time they are stirred every 6 h to evaporate the unabsorbed water.

To determine the true moisture content of wheat samples, the national standard method of China (i.e., GB5497-85) is utilized. Table 1 shows the 10 sets of real moisture level, where M_{target} denotes the target levels, and M_{real} denotes the real moisture content detected by the national standard method (as ground truth). Due to experimental errors and other factors, the results are a little different from the target M_{target}, as given in the *Error* Row. It is clear tat the errors are all pretty minor.

5.2. Optimal parameter setting

For optimal performance, the factors of embedding dimension m and scaling t should be properly specified throughout the CSI data reconstruction process. The parameters m and t should be neither too high nor too small in order to reduce information redundancy and capture more signal characteristics. In fact, there is no existing method for determining the most suitable values. Thus, in this section, we aim to find the optimal parameter setting through experiments.

Figs. 7–10 show the entropy at different dimensions m, when the scaling factor t is set to 1. These figures illustrate the process of determining the optimal embedding dimension m. The value of m is increased from 3 to 15. After numerous attempts, we discovered that as m is increased gradually, the resolution of entropy becomes smaller and smaller. The boxes in Figs. 9 and 10 represent wheat moisture level indices with equal or similar entropy values, indicating that these moisture levels are difficult to classify. It can be inferred that $m = 3$ or $m = 5$ appear to be more appropriate, since the 10 types of wheat moisture levels can be easily distinguished with these settings.

Figs. 11–14 demonstrate the influence of the scaling factor t on entropy when the embedding dimension m is fixed to 5. After many attempts, the value of m is set to 5 to find the best scaling factor t. In order to facilitate better observations, we rearrange the moisture level index in these experiments. Fig. 11 shows that there are two moisture level indices, i.e., 6 and 7, which are hard to distinguish when $t = 2$. Fig. 13 shows that it is hard to distinguish indices 4 from 5 when $t = 5$, and Fig. 14 shows that it is hard to distinguish indices 5 from 6 to 9 from 10 when $t = 8$. However, Fig. 12 shows that all the 10 entropy values can be distinguished when $t = 3$ and $m = 5$.

Table 2 shows the entropy of the CSI data for 10 different varieties of wheat samples at different moisture levels, computed according to (9)–(13). In Table 2, MCSEn_1 to MCSEn_10 are the MCSEn for wheat samples 1 to 10, respectively. The 56 subcarriers of the WiFi channel are represented by Subcarrier_1 to Subcarrier_56. The entropy data presented in the table will be utilized for training the multi-class SVM model. For a better illustration of the entropy data, we also plot it in Fig. 15, where the 10 curves represent 10 moisture content levels, respectively. The marked rectangles in the figure indicate many intersections of the

Table 1
Error between the adjusted moisture content levels and the target moisture content levels.

	Level 1	Level 2	Level 3	Level 4	Level 5	Level 6	Level 7	Level 8	Level 9	Level 10
M_{target}	8.0%	9.0%	10.0%	11.0%	12.0%	13.0%	14.0%	15.0%	16.0%	17.0%
M_{real}	8.2%	9.6%	10.3%	11.2%	12.0%	13.0%	14.6%	15.6%	16.8%	17.7%
Error	0.2%	0.6%	0.3%	20.0%	0%	0%	0.6%	0.6%	0.8%	0.7%

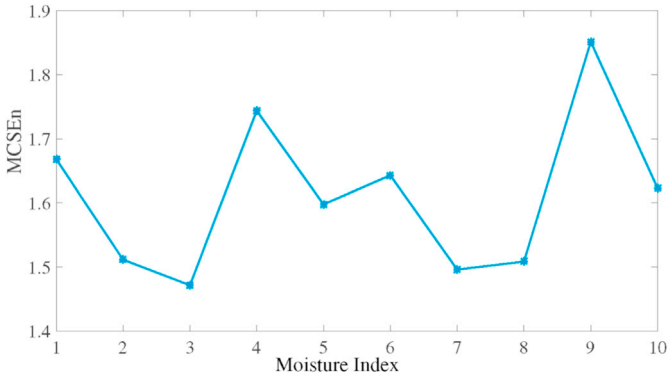

Fig. 7. Entropy with embedded dimension $m = 3$.

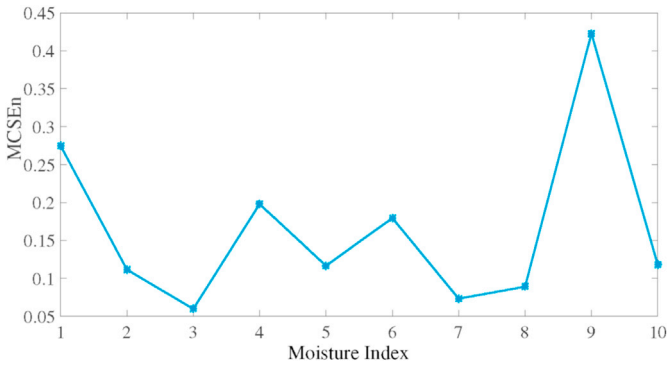

Fig. 8. Entropy with embedded dimension $m = 5$.

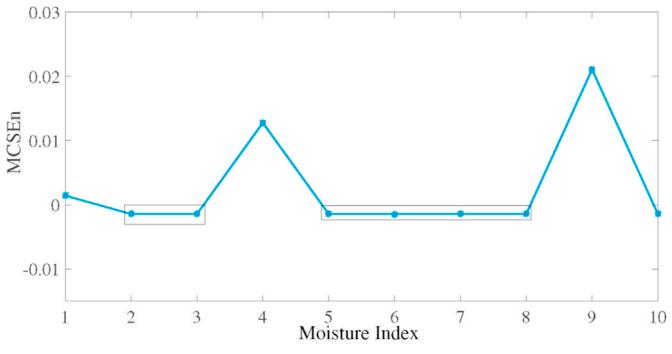

Fig. 9. Entropy with embedded dimension $m = 8$.

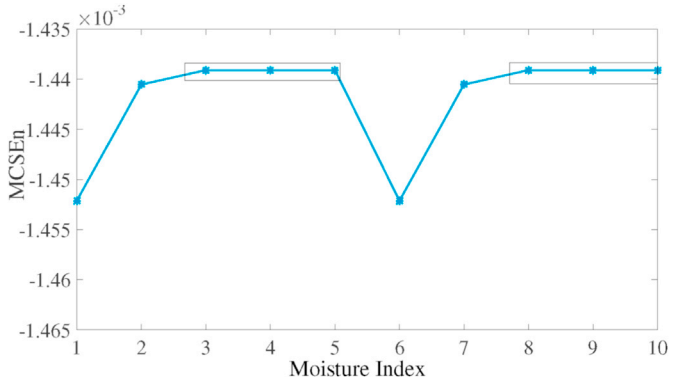

Fig. 10. Entropy with embedded dimension $m = 15$.

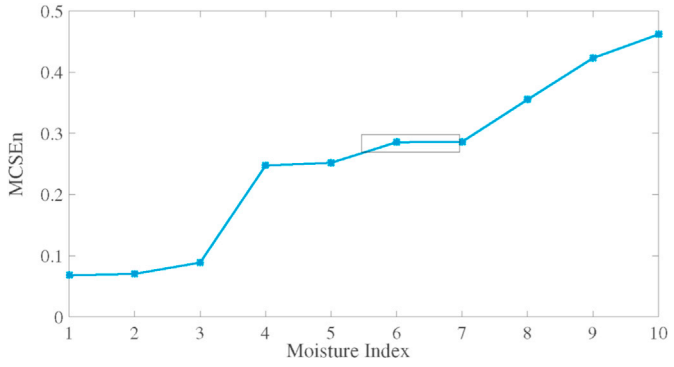

Fig. 11. Entropy with scale $t = 2$ and dimension $m = 5$.

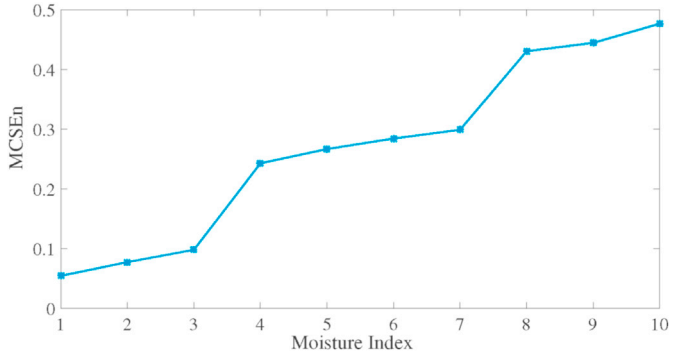

Fig. 12. Entropy with scale $t = 3$ and dimension $m = 5$.

entropy curves, meaning these moisture levels cannot be classified correctly. As a result, it is considered necessary to utilize multiple antennas for more accurate identification.

5.3. Entropy of subcarriers on different antennas

Although the best factors m and t are determined, we still cannot use the signal entropy of any subcarrier and any receiving antenna to classify the wheat samples. Because of the fine-grained characteristics of the CSI data, changes in the external environment have a great impact on the CSI. As a result, we will continue to examine the influence of different antennas and subcarriers on entropy. Subcarrier 4 and subcarrier 35 on antenna 2 are randomly selected for a comparison study, and the results are shown in Figs. 16 and 17.

It can be seen that moisture indices 6 and 7 have almost the same entropy value on subcarrier 4. In contrast, the entropy of subcarrier 35 from the same antenna can better distinguish moisture indices 6 and 7. However, as shown in Fig. 17, the entropy of subcarrier 35 on antenna 2 does not distinguish between moisture indices 8 and 9. Figs. 18 and 19 show the entropy of subcarrier 4 and subcarrier 35 on antenna 3, respectively. There are still three moisture indices, namely, 4, 5, and 6,

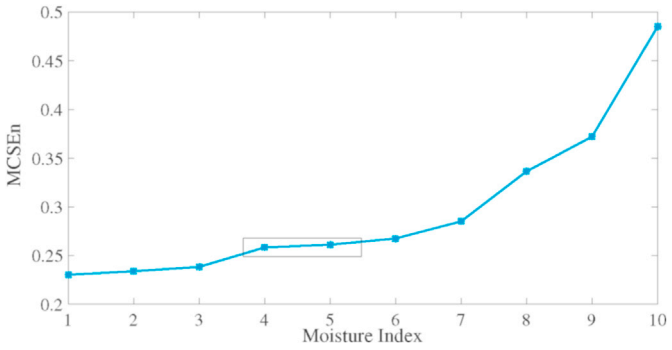

Fig. 13. Entropy with scale $t = 5$ and dimension $m = 5$.

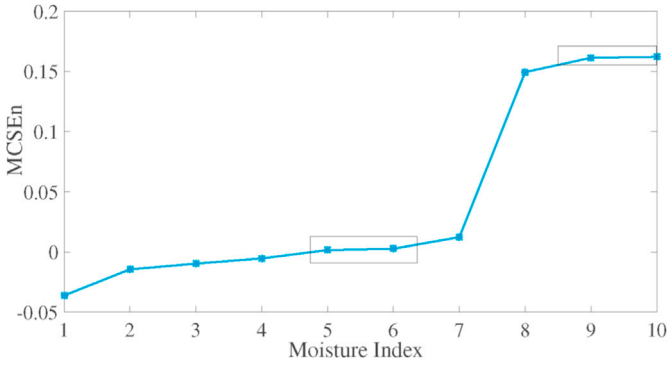

Fig. 14. Entropy with scale $t = 8$ and dimension $m = 5$.

having the same or similar entropy values for subcarrier 35, as shown in Fig. 19. However, the entropy values of subcarrier 4 on the antenna can differentiate all the 10 moisture indices. As a result, it is clear that using only one CSI subcarrier entropy from a single antenna makes it difficult to reliably identify moisture levels.

Fig. 20 plots the mean entropy values of all 56 subcarriers on all three receiving antennas. It is expected to achieve accurate classification by using the mean entropy values. However, it can be seen that there are still two sets of indices, i.e., indices 2 and 3, and indices 4 and 5, which are hard to classify. As a result, using the mean entropy does not help much to achieve an accurate classification.

Through the above studies, we make the following observations:

- using the entropy from a single subcarrier on a single antenna would not accurately classify wheat moisture levels;
- using the entropy from a single subcarrier on multiple antennas would also not accurately classify wheat moisture levels;
- the entropy from a single antenna with multiple subcarriers could be used to classify the 10 types of wheat moisture levels, but the accuracy may be poor;

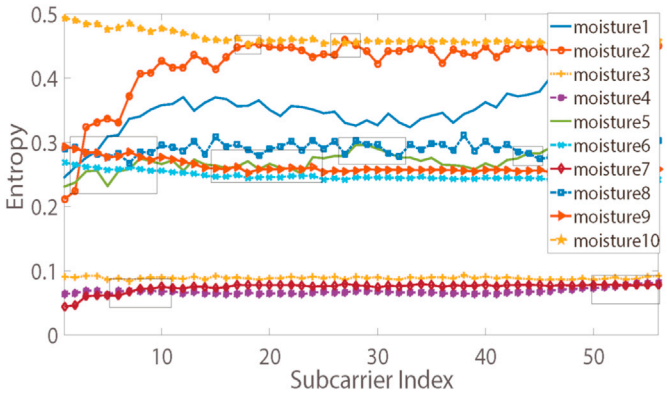

Fig. 15. Entropy of the CSI data collected from the 56 subcarriers of the WiFi channel for 10 different wheat moisture levels.

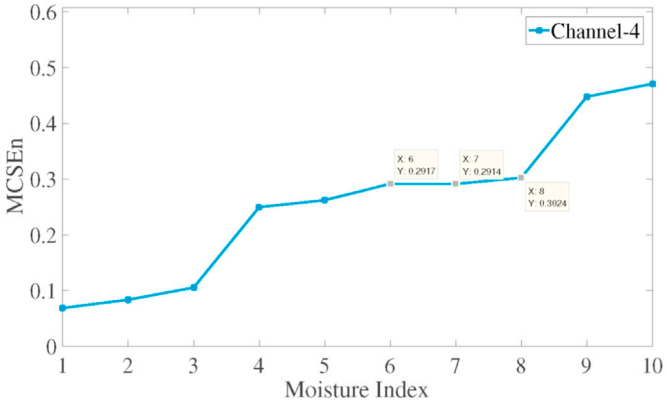

Fig. 16. Entropy of subcarrier 4 on antenna 2.

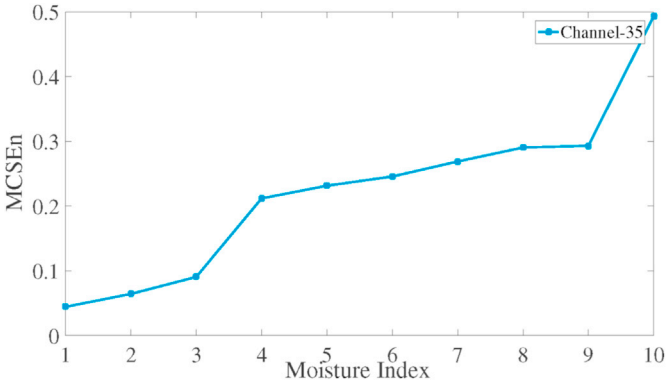

Fig. 17. Entropy of subcarrier 35 on antenna 2.

Table 2
Entropy of the CSI data collected from the 56 subcarriers in the LOS scenario for 10 wheat samples at different moisture levels.

	MCSEn_1	MCSEn_2	MCSEn_3	MCSEn_4	MCSEn_5	MCSEn6	MCSEn_7	MCSEn_8	MCSEn_9	MCSEn_10
Subcarrier_1	0.2455	0.2116	0.0904	0.0641	0.2312	0.2687	0.0442	0.2903	0.2930	0.4930
Subcarrier_2	0.2616	0.2243	0.0896	0.0648	0.2373	0.2653	0.0462	0.2925	0.2903	0.4903
Subcarrier_3	0.2758	0.3232	0.0918	0.0690	0.2546	0.2620	0.0602	0.2834	0.2844	0.4844
Subcarrier_4	0.2863	0.3311	0.0923	0.0685	0.2561	0.2611	0.0613	0.2820	0.2840	0.4840
Subcarrier_5	0.3090	0.3372	0.0860	0.0625	0.2319	0.2572	0.0616	0.2768	0.2764	0.4764
Subcarrier_6	0.3114	0.3303	0.0886	0.0683	0.2548	0.2577	0.0611	0.2832	0.2785	0.4785
Subcarrier_7	0.3365	0.3721	0.0841	0.0681	0.2583	0.2611	0.0668	0.2675	0.2851	0.4851
…	…	…	…	…	…	…	…	…	…	…
Subcarrier_56	0.4216	0.4503	0.0914	0.0819	0.3839	0.2424	0.0783	0.3024	0.2582	0.4582

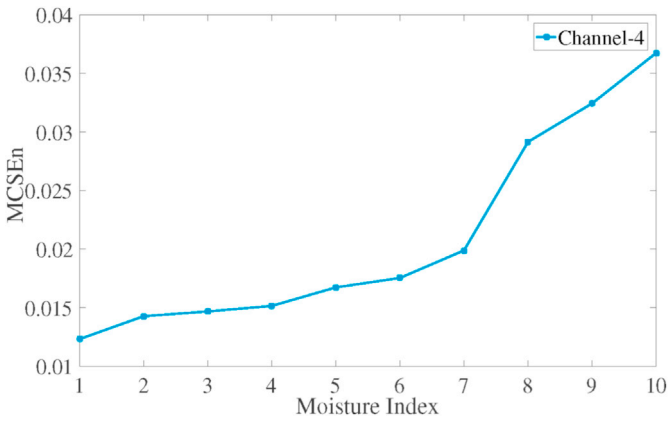

Fig. 18. Entropy of subcarrier 4 on antenna 3.

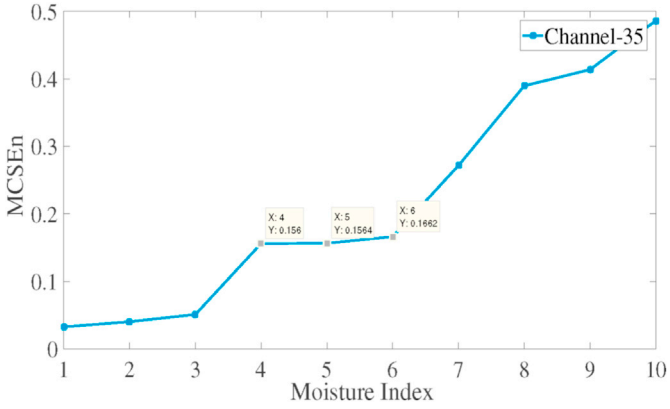

Fig. 19. Entropy of subcarrier 35 on antenna 3.

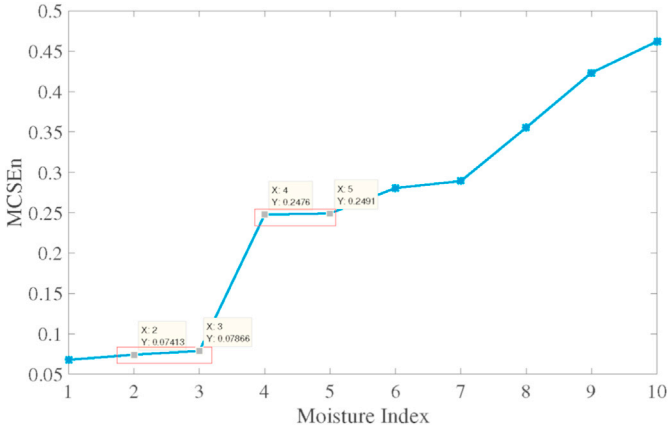

Fig. 20. The mean entropy values over all the 56 subcarriers from all the three antennas.

- using the entropy from multiple antennas and multiple subcarriers can accurately classify the 10 types of wheat moisture levels.

The fine-grained CSI data also contains considerable external interference since only part of the WiFi signal penetrates the wheat box. Thus, if we only consider a chosen subcarrier or a single antenna, we may lose much useful information. As a result, all the subcarriers on all the receiving antennas should be utilized to classify wheat moisture levels to achieve a high classification accuracy. The Multi-class SVM algorithm is proposed to utilize all the entropy information from all the subcarriers and antennas.

5.4. Accuracy of Wi-Wheat+

For each CSI sample in this experiment, the data structure is as $1 \times 3 \times 56 \times 1000$, which represents one transmitting antenna, three receiving antennas, 56 subcarriers, and 1000 received packets. There are 10 types of wheat samples used, each at a different moisture level as given in Table 3. Wi-Wheat+ calculates the MCSEn of each wheat signal from each subcarrier, and then the data structure of $3 \times 56 \times 10$ is obtained. In each experiment, we obtain 168×10 entropy characteristic samples. We repeat the experiment five times yielding 840×10 groups of samples. The samples are randomly divided into three sets: the first part (60%) is used to train the multi-class SVM model; the second part (20%) is used to train the model using noisy data to make it more robust; and the third part (20%) is used to test the trained model.

Table 3 shows the classification targets from moisture level index M1 to moisture level index M10, which are used as labels for the Multi-class SVM. The oven drying method is used to prepare the wheat samples to the target moisture content. In the table, symbols M1 to M10 represent the 10 different wheat moisture levels, respectively.

The linear kernel function, polynomial kernel function, and Gaussian RBF, among others, are the most commonly used kernel functions in SVM. Table 4 shows the outcomes of our experiments with three different kernel functions for the LOS situation. When applied to the same training and testing data, the Gaussian RBF has the highest classification accuracy of the three, while the polynomial kernel function has the lowest. As a result, we use the Gaussian RBF in Wi-Wheat+.

We also examined the NLOS case. Table 5 summarizes the computed MCSEn values for the 56 subcarriers for the 10 types of wheat samples. The entropy data is then used to train the Multi-class SVM model and is used for the classification of new sample data. Table 6 shows the classification accuracy in the NLOS scenario. As may be seen, classification accuracy results are also quite satisfactory. Similarly, the Gaussian RBF kernel function achieves the highest accuracy of the three kernel functions, whereas the polynomial kernel function has the poorest performance, except for M9 and M10.

Fig. 21 shows the accuracy of wheat moisture prediction in the LOS and NLOS scenarios with the Wi-Wheat+ system compared. It is clear that the classification accuracy in the LOS scenario is higher than in the NLOS situation. We hypothesize that this is because, in the event of LOS, the received signal contains more components passing through the wheat box, which more accurately captures the characteristics of wheat moisture content and helps the Multi-class SVM better classify the wheat samples.

6. Conclusions

In this paper, we propose the Wi-Wheat+ system that utilizes commodity WiFi to sense CSI data and estimate grain moisture content level. The captured WiFi CSI data was first calibrated. Then the algorithm of MCSEn was proposed to extract the features related to grain moisture

Table 3
Classification label: Moisture indices of 10 different wheat samples.

Moisture Index 1 – Index 10									
M1	M2	M3	M4	M5	M6	M7	M8	M9	M10
8.2%	9.6%	10.3%	11.2%	12.0%	13.0%	14.6%	15.6%	16.8%	17.7%

Table 4
Classification accuracy in the LOS scenario (%).

	M1	M2	M3	M4	M5	M6	M7	M8	M9	M10
Gaussian Radial Basis Function (RBF)	100	93	91	100	98	93	96	99	100	100
Linear Kernel Function	94	87	87	92	89	91	87	86	95	98
Polynomial Kernel Function	89	86	88	89	92	94	91	95	91	95

Table 5
Entropy of the CSI data collected from the 56 subcarriers in the NLOS scenario for 10 wheat samples at different moisture levels.

	MCSEn_1	MCSEn_2	MCSEn_3	MCSEn_4	MCSEn_5	MCSEn_6	MCSEn_7	MCSEn_8	MCSEn_9	MCSEn_10
Subcarrier_1	0.5229	0.3176	0.3169	0.8420	1.2743	0.7424	0.6780	0.5129	0.4875	0.4628
Subcarrier_2	0.4919	0.3725	0.3467	0.8244	1.2488	0.7791	0.7570	0.6148	0.5158	0.4904
Subcarrier_3	0.4255	0.3932	0.3297	0.5835	1.1872	0.6737	0.6000	0.4130	0.4916	0.7826
Subcarrier_4	0.3863	0.3638	0.2804	0.5599	0.9627	0.5704	0.5606	0.4497	0.4908	1.1968
Subcarrier_5	0.3274	0.2721	0.3377	0.5747	0.7921	0.5827	0.5535	0.5038	0.3862	1.2508
Subcarrier_6	0.4796	0.3549	0.3553	0.8029	0.8770	0.6790	0.5298	0.5629	0.5481	1.4363
Subcarrier_7	0.4005	0.3845	0.2860	0.5835	0.6980	0.5703	0.4896	0.4015	0.4348	1.4053
…	…	…	…	…	…	…	…	…	…	…
Subcarrier_56	0.4719	0.3652	0.3557	0.5298	0.7887	0.6096	0.7065	0.5544	0.3898	0.9168

Table 6
Classification accuracy of the NLOS scenario (%).

	M1	M2	M3	M4	M5	M6	M7	M8	M9	M10
Gaussian Radial Basis Function	99	91	98	98	94	94	95	98	96	97
Linear Kernel Function	87	88	92	88	95	91	90	89	85	86
Polynomial Kernel Function	83	88	89	85	90	85	87	95	94	91

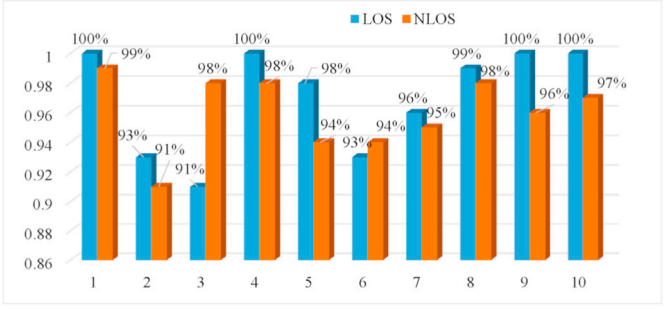

Fig. 21. Comparison of classification accuracy in the LOS and NLOS scenarios.

content, which was fed into a multi-class SVM to establish the multi-classification model of moisture prediction. The feasibility of the proposed Wi-Wheat+ system was validated with experiments using real wheat samples in both LOS and NLOS scenarios with a satisfactory classification accuracy.

Declaration of competing interest

The fourth author of this paper, Dr. Shiwen Mao, is an associate editor of DCN.

Acknowledgments

This work is supported in part by the Program for Science & Technology Innovation Talents in Universities of Henan Province (19HASTIT027), National Natural Science Foundation of China (62172141), Zhengzhou Major Scientific and Technological Innovation Project (2019CXZX0086), Youth Innovative Talents Cultivation Fund Project of Kaifeng University in 2020 (KDQN-2020-GK002), the National Key Research and Development Program of China (2017YFD0401001), the NSFC (61741107), the NSF (CNS-2105416), and by the Wireless Engineering Research and Education Center at Auburn University.

References

[1] D.S. Jayas, Storing grains for food security and sustainability, Agric. Res. 1 (1) (Mar. 2012) 21–24.
[2] S.O. Nelson, S. Trabelsi, Historical development of grain moisture measurement and other food quality sensing through electrical properties, IEEE Instrum. Meas. Mag. 19 (1) (Jan. 2016) 16–23.
[3] S.O. Nelson, Sensing moisture content in grain, IEEE Instrum. Meas. Mag. 3 (1) (Mar. 2000) 17–20.
[4] D. Vasisht, et al., FarmBeats: an IoT platform for data-driven agriculture, in: Proc. USENIX NSDI'17, Boston, MA, Mar. 2017, pp. 515–529.
[5] American Society of Agricultural Engineers, Moisture Measurement–Unground Grain and Seeds, ASAE Standard, Dec. 2001, pp. 67–568.
[6] W. Wang, Y. Dai, A grain moisture detecting system based on capacitive sensor, Int. J. Digital Content Technol. Appl. 5 (3) (Mar. 2011) 203–209.
[7] F. Gan, Z. Liu, W. Zhang, M. Li, R. Wang, J. Feng, Development of grain moisture detecting instrument based on friction resistance method, J. Agric. Mech. Res. 40 (1) (Jan. 2018) 91–95.
[8] Z. Liu, et al., Research on online moisture detector in grain drying process based on V/F conversion, Hindawi Math. Problems Eng. 2015 (2015), 565764. Article ID.
[9] S.O. Nelson, A.W. Kraszewski, S. Trabelsi, K.C. Lawrence, Using cereal grain permittivity for sensing moisture content, IEEE Trans. Instrum. Meas. 49 (3) (June 2000) 470–475.
[10] K. Kim, J. Kim, C. Lee, S. Noh, M. Kim, Simple instrument for moisture measurement in grain by free-space microwave transmission, Trans. ASABE (Am. Soc. Agric. Biol. Eng.) 49 (4) (2006) 1089–1093.
[11] Y. Yang, J. Wang, C. Wang, et al., Study on on-line measurement of grain moisture content by neutron gauge, Trans. Chin. Soc. Agric. Eng. 16 (5) (May 2000) 99–101.
[12] D. Nath K, P. Ramanathan, P. Ramanathan, Non-destructive methods for the measurement of moisture contents–a review, Sens. Rev. 37 (1) (Jan. 2017) 71–77.
[13] H. Zhu, F. Xiao, L. Sun, X. Xie, R. Wang, CSI-based Wi-Fi environment sensing, J. Nanjing Univ. Posts Telecommun. (Nat. Sci. Ed.) 36 (1) (Feb. 2016) 95–103.
[14] X. Wang, X. Wang, S. Mao, RF sensing for Internet of Things: a general deep learning framework, IEEE Commun. Mag. 56 (9) (Sept. 2018) 62–67.
[15] Z. Yang, Z. Zhou, Y. Liu, From RSSI to CSI: indoor localization via channel response, ACM Comput. Surv. 46 (2) (Nov. 2013) 25.
[16] W. Yang, X. Wang, A. Song, S. Mao, Wi-Wheat: contact-free wheat moisture detection with commodity WiFi, in: Proc. IEEE ICC'18, Kansas City, MO, May 2018, pp. 1–6.
[17] O. Stuart, S.T. Nelson, Principles for microwave moisture and density measurement in grain and seed, J. Microw. Power Electromagn. Energy 39 (2) (Feb. 2004) 107–117.
[18] J. Xiao, K. Wu, Y. Yi, L.M. Ni, FIFS: fine-grained indoor fingerprinting system, in: Proc. ICCCN'12, Munich, Germany, Aug. 2012, pp. 1–7.
[19] X. Wang, L. Gao, S. Mao, S. Pandey, CSI-based fingerprinting for indoor localization: a deep learning approach, IEEE Trans. Veh. Technol. 66 (1) (Jan. 2017) 763–776.

[20] X. Wang, L. Gao, S. Mao, CSI phase fingerprinting for indoor localization with a deep learning approach, IEEE Internet Things J. 3 (6) (Dec. 2016) 1113–1123.
[21] X. Wang, L. Gao, S. Mao, BiLoc: Bi-modality deep learning for indoor localization with 5GHz commodity Wi-Fi, IEEE Access J. 5 (1) (Mar. 2017) 4209–4220.
[22] X. Wang, X. Wang, S. Mao, Indoor fingerprinting with bimodal CSI tensors: a deep residual sharing learning approach, IEEE Internet Things J. 8 (6) (Mar. 2021) 4498–4513.
[23] X. Wang, X. Wang, S. Mao, Deep convolutional neural networks for indoor localization with CSI images, IEEE Trans. Netw. Sci. Eng. 7 (1) (Jan./Mar. 2020) 316–327.
[24] Y. Wang, et al., E-Eyes: device-free location-oriented activity identification using fine-grained WiFi signatures, in: Proc. ACM MobiCom'14, Maui, HI, Sept. 2014, pp. 617–628.
[25] G. Wang, Y. Zou, Z. Zhou, K. Wu, L. Ni, We can hear you with Wi-Fi, in: Proc. ACM MobiCom'14, Maui, HI, Sept. 2014, pp. 593–604.
[26] W. Wang, A. Liu, M. Shahzad, K. Ling, S. Lu, Understanding and modeling of WiFi signal based human activity recognition, in: Proc. ACM MobiCom'15, Paris, France, Sept. 2015, pp. 65–76.
[27] Y. Wang, K. Wu, L.M. Ni, WiFall: device-free fall detection by wireless networks, IEEE Trans. Mobile Comput. 16 (2) (Feb. 2017) 581–594.
[28] H. Wang, et al., RT-Fall: a real-time and contactless fall detection system with commodity WiFi devices, IEEE Trans. Mobile Comput. 16 (2) (Feb. 2017) 511–526.
[29] X. Wang, C. Yang, S. Mao, PhaseBeat: exploiting CSI phase data for vital sign monitoring with commodity WiFi devices, in: Proc. IEEE ICDCS'17, Atlanta, GA, June 2017, pp. 1230–1239.
[30] X. Wang, C. Yang, S. Mao, TensorBeat: tensor decomposition for monitoring multi-person breathing beats with commodity WiFi, ACM Trans. Intell. Syst. Technol. 9 (1) (Sept. 2017) 8.1–8.27.
[31] S. Zhong, Y. Huang, R. Ruby, L. Wang, Y.-X. Qiu, K. Wu, Wi-Fire: device-free fire detection using WiFi networks, in: Proc. IEEE ICC'17, Paris, France, May 2017, pp. 1–6.
[32] K. Wu, Wi-Metal: detecting metal by using wireless networks, in: Proc. IEEE ICC'16, Kuala Lumpur, Malaysia, May 2016, pp. 1–6.
[33] Z. Zhou, Z. Yang, C. Wu, et al., LiFi: line-of-sight identification with WiFi, in: Proc. IEEE INFOCOM'14, Toronto, Canada, Apr.-May 2014, pp. 2688–2696.
[34] W. Yang, X. Wang, S. Cao, H. Wang, S. Mao, Multi-class wheat moisture detection with 5GHz Wi-Fi: a deep LSTM approach, in: Proc. 2018 International Conference on Computer Communication and Networks (ICCCN'18), Hangzhou, China, July/Aug. 2018, pp. 1–8.
[35] J.A. Suykens, J. Vandewalle, Least squares support vector machine classifiers, Neural Process. Lett. 9 (3) (June 1999) 293–300.
[36] C.-C. Chang and C.-J. Lin, "LIBSVM – A Library for Support Vector Machines," [online] Available: https://www.csie.ntu.edu.tw/∼cjlin/libsvm/.
[37] Y. Gong, T. Yang, Y. Liang, Integrating ultra weak luminescence properties and multi-scale permutation entropy algorithm to analyze freshness degree of wheat kernel, Elsevier Optik J. 218 (Sept. 2020), 165099.
[38] P. Hu, W. Yang, X. Wang, S. Mao, MiFi: device-free wheat mildew detection using off-the-shelf WiFi devices, in: Proc. IEEE GLOBECOM'19, Waikoloa, HI, Dec. 2019, pp. 1–6.